Self-organization of nanoparticles and molecules in periodic Liesegang-type structures

April 30 2021, by Thamarasee Jeewandara

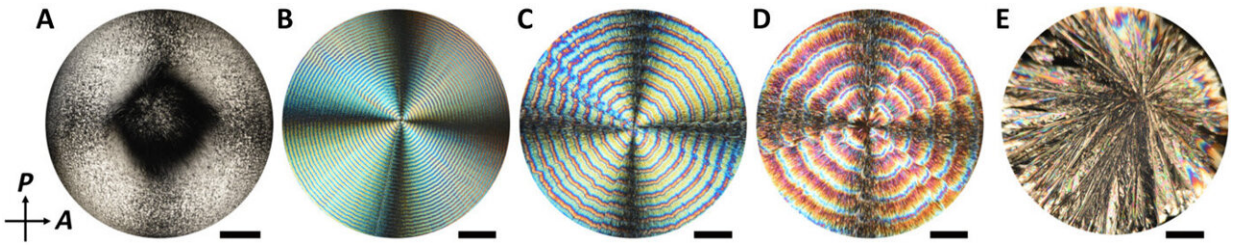

Polarizing Optical Microscopy (POM) images of CNC, TA/CNC, and TA films. POM images of films formed from (A) a CNC suspension; (B to D) TA/CNC suspensions with (left to right) R of 4.0, 5.0, and 6.0; and (E) a TA solution. Films were formed at 22°C and RH = 23%. The concentration of CNCs in (A) to (D) was 3 wt %, and the concentration of TA solution in (E) was 11.3 wt % (750 mM). All films were dried for 24 hours. Scale bars, 420 μm. Credit: Science Advances, doi: 10.1126/sciadv.abe3801

Chemical organization in reaction-diffusion systems offer a strategy to generate materials with ordered morphologies and architecture. Periodic structures can be formed using molecules or nanoparticles. An emerging frontier in materials science aims to combine nanoparticles and molecules. In a new report on *Science Advances*, Amanda J. Ackroyd and a team of scientists in chemistry, physics and nanomaterials in Canada, Hungary and the U.S. noted how solvent evaporation from a suspension

of cellulose nanocrystals (CNCs) and L-(+)-tartaric acid [abbreviated L-(+)-TA] caused the phase separation of precipitation to result in the rhythmic alteration of CNC-rich, L-(+)-TA rings. The CNC-rich regions maintained a cholesteric structure, while the L-(+)-TA-rich bands formed via radially elongated bundles to expand the knowledge of self-organizing reaction-diffusion systems and offer a strategy to design self-organizing materials.

Chemical organization

The process of self-organization and self-assembly occurs universally in non-equilibrium systems of living matter, geochemical environments, materials science and in industry. Existing experiments that lead to periodic structures can be divided into two groups including the classical Liesegang-type experiments and chemical organization via periodic precipitation to generate materials with ordered morphologies and structural hierarchy. In this work, Ackroyd et al. developed a strategy for solvent evaporation to phase separate an aqueous solution of tartaric acid/cellulose nanocrystals [L-(+)-TA/CNC or TA/CNC] for its subsequent precipitation to result in a rhythmic alternation of CNC-rich or CNC-depleted ring-type regions. The team developed a kinetic model which agreed with the experimental results quantitatively. The work expands the range of self-organizing reaction-diffusion systems to pave the way for periodically structured functional materials.

Experiments

Ackroyd et al. deposited mixed suspensions as droplets on glass slides and immediately placed them in a humidity chamber. Using a polarizing optical microscope (POM), they formed images of the drying films with varying TA/CNC (tartaric acid/cellulose nanocrystals) compositions. Films formed by drying the tartaric acid solution maintained a spherulite morphology with a needle-like structure. Using images of drying

TA/CNC, the team noted the formation of rings beginning from a nucleation point close to the film center from which periodic and grew radially towards the edge of the film. They then characterized the ring patterns in the films, where the increasing relative humidity, increased the value of their period. To understand the growth dynamics of the formation of periodic rings, Ackroyd et al. recorded the evolution of the spatio-temporal patterns of water evaporation for the liquid films. They labeled CNCs with a covalently attached fluorescein isothiocyanate (FITC) dye, to characterize the composition of alternating rings in the composite film. Based on the POM (polarizing optical microscope) images, they noted the CNC-enriched and CNC-deprived periodic bands in the composite film.

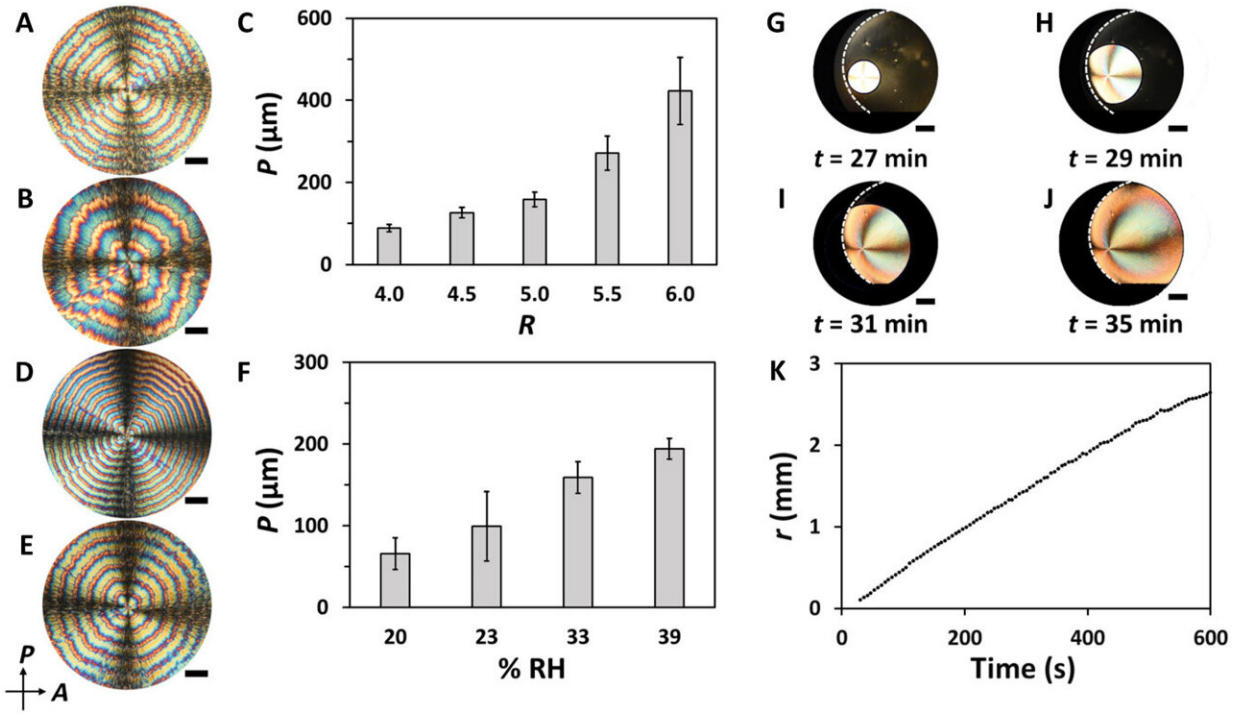

Characterization of ring patterns in TA/CNC films. (A and B) POM images of films formed at R of 4.5 (A) and 5.5 (B). (C) Variation in the average period, P, of the ring pattern, plotted as a function of R. In (A) to (C), films were formed at RH = 33%. (D and E) POM images of films formed at RH = 23% (D) and 33%

(E). (F) Variation in the average period, P, of the ring pattern, plotted as a function of RH. (D to F) Films were formed at R = 5.0. Error bars in (C) and (F) represent SDs for nine samples. Scale bars (A, B, D, and E), 300 μm. (G to J) POM images of a liquid TA/CNC film (R = 4.5, RH ≈ 21%), taken at various drying times. The white dashed lines show the outline of the drying droplet circumference. (K) Variation in the distance, r, from the nucleation point to the outer edge of the drying film, plotted as a function of time. Scale bars (G to J), 500 μm. Credit: Science Advances, doi: 10.1126/sciadv.abe3801

Characterizing the composite film.

To characterize the composite films further, the scientists acquired spectra under differential transmission of circularly polarized light of opposite handedness. Using scanning electron microscopy, they obtained images of the film cross-section of the CNC-rich and TA-rich regions. To understand the topography of the surface of the composite film, they used atomic force microscopy. Using high-magnification POM images, Ackroyd et al. noted the TA-rich regions in yellow and light orange, while the CNC-rich regions appeared red and green in color. The team also conducted polarimetry imaging to map the variation in the polarization state of transmitted light. To accomplish this, they illuminated a film with a 532 nm linearly polarized light with a light polarization state set parallel to the vertical edge of the images. Based on both POM and polarimetry experiments, Ackroyd et al revealed the orientation order in TA-rich ring-banded regions relative to the chemical composition of the film. The structural features formed by CNCs and TA provided an interesting example of complex, out-of-equilibrium organization, of interest for future studies. To probe the TA/CNC films in the transmission mode, the scientists also used small-angle X-ray scattering, where an X-ray beam size of 220 x 50 μm allowed an entire film to be scanned for mapping with the technique.

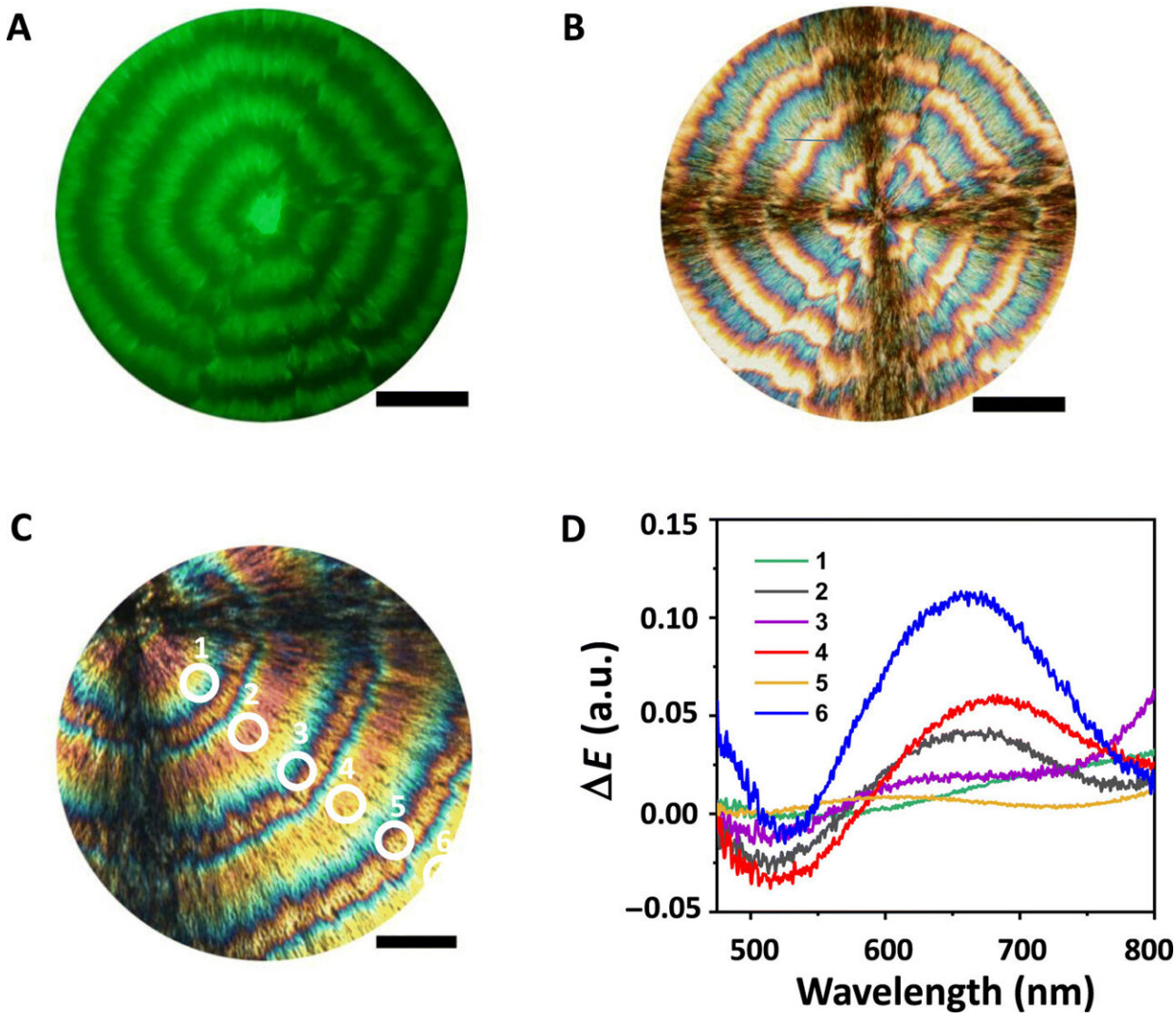

Characterization of the composition of periodic bands in the composite film. (A) Fluorescence microscopy and (B) POM images of TA/FITC-CNC films formed at R = 5.0 and RH = 33%. Scale bars (A and B), 150 μm. (C and D) The variation in ΔE of the TA-rich bands (labeled as 1, 3, and 5) and CNC-rich bands (labeled as 2, 4, and 6) in (C). The ΔE spectra in (D) are collected from the regions marked in (C). Scale bar (C), 100 μm. a.u., arbitrary units. Credit: Science Advances, doi: 10.1126/sciadv.abe3801

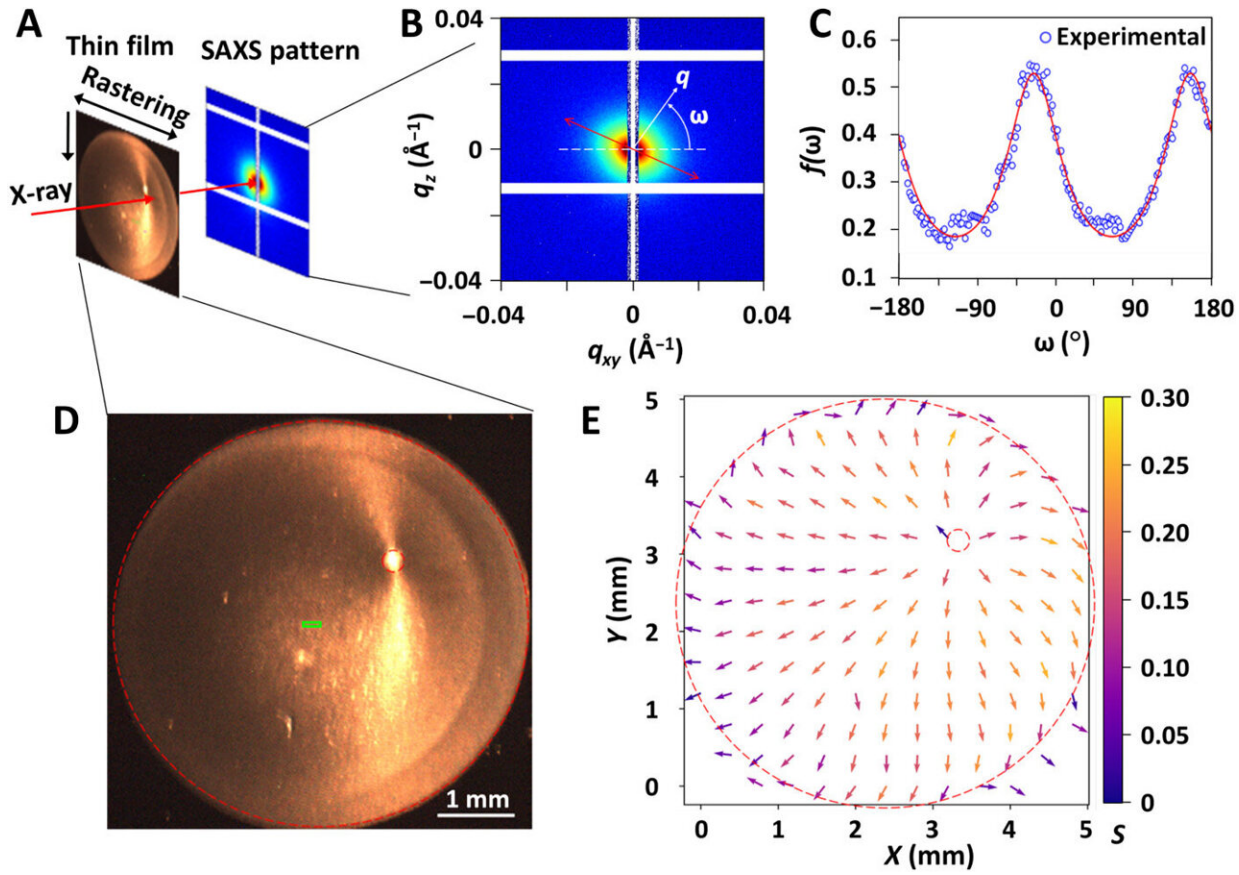

Characterization of local anisotropy of the TA/CNC film by SAXS. (A) Schematic illustration of the SAXS rastering measurement for SAXS mapping of the film. (B) A typical SAXS pattern with a definition of the azimuthal angle ω. (C) 2D ODF f(ω), calculated from the SAXS pattern in (B), shows the anisotropic features along the most probable angle, denoted by ω0, which provides information about the orientation within the film. The value of f(ω) is fitted using an ad hoc order parameter (red curve), described in section S9. (D) A photograph of the film taken during the SAXS measurement with dashed circles showing the circular edge of the dried droplet and the center of the concentric rings. The green rectangular box in the center of the film represents the size and shape of the x-ray beam. (E) Orientations of anisotropic scatterers, probed by the SAXS measurements and mapped on the entire area of the film. The direction of each arrow indicates the orientation in that location. The color represents the orientation order parameter in 2D, termed S, with the scale shown on the right. The dashed circles correspond to the circular edge of the film and the center of the concentric rings, similar to those shown in (D). The film was

prepared at R = 5.0 and RH = 23%. Credit: Science Advances, doi: 10.1126/sciadv.abe3801

Numerical model

The scientists then developed a kinetic model for the phase-separating TA/CNC suspension as applied generally to reaction-diffusion systems. They represented the dynamics of the periodic pattern formation with two types of building blocks using a set of differential equations. The numerical model factored six species of the drying TA/CNC suspension including the (1) dissolved TA, (2) the nuclei of precipitated TA, (3) the crystals of TA in the TA-rich phase and the (4) the suspended individual CNCs, (5) the TA-CNC clusters, and 6) the CNC-enriched phase. The numerical model qualitatively reproduced the experimental findings, and the model predicted a finite constant velocity of the moving front of the edge pattern.

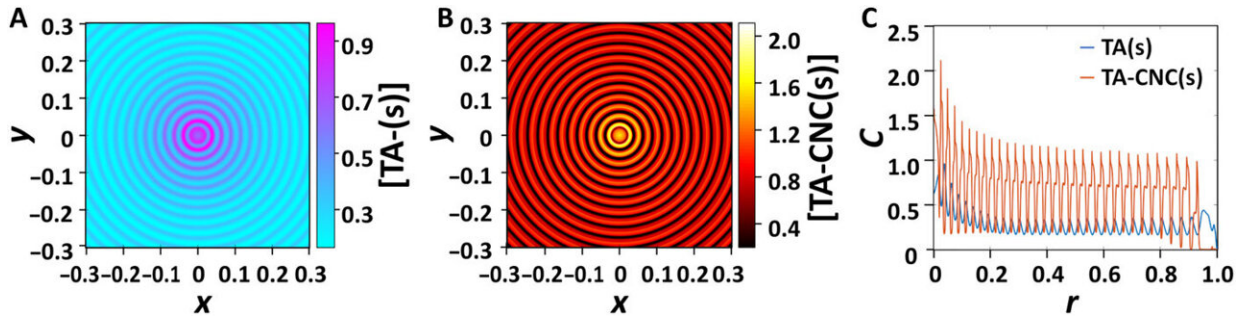

Numerical simulations of ring pattern formation. (A) Spatial distribution of TA-(s), (B) spatial distribution of CNCs, and (C) concentration profiles of TA and CNCs in alternating ring-type bands. In the simulations, the following parameters were used: DA = 10−1, DB = 10−2, DD = 10−2, DE = 10−4, d* = 0.8, and e* = 0.2. The grid spacing (Δr) and time step (Δt) in the numerical simulations were 10−3 and 1.8 × 10−8. All parameters and variables are in

dimensionless units. Credit: Science Advances, doi: 10.1126/sciadv.abe3801

Outlook

In this way, Amanda J. Ackroyd and colleagues provided first evidence of a periodic ring-banded structure formed by two components with dimensions differing by several orders of magnitude. The results differed from ring patterns obtained by other phenomena including "coffee ring" patterns. The scientists noted the evaporation of water from the TA/CNC suspension to result in the saturation of CNCs and TA in the mixture. They controlled the morphology of the composite films by varying the composition of the TA/CNC suspension and relative humidity. Based on simulations, the team noted that the periodic ring patterns did not qualitatively change with increasing viscosity and therefore reduced the diffusion coefficients of the compounds. They highlighted distinct band structures for the CNC-enriched and TA-enriched ring-banded regions throughout the study. The work will expand the knowledge of self-organizing reaction-diffusion systems and provide strategies to design self-organizing materials.

More information: Ackroyd J. et al. Self-organization of nanoparticles and molecules in periodic Liesegang-type structures, *Science Advances*, 10.1126/sciadv.abe3801

Epstein I.R. and Xu B. Reaction–diffusion processes at the nano- and microscales, *Nature Nanotechnology*, doi.org/10.1038/nnano.2016.41

Anderson L.C. et al. Morphology of poly-L-alanine spherulites. *Nature*, doi.org/10.1038/216052a0